

An in-line in-fibre ring cavity multi-parameter sensor with a tunable refractive index response

Author:

Childs, Paul; Leung, Ian; Wong, Allan; Peng, Gang-Ding

Publication details:

Photonics Asia 2007: Sensors and Imaging

Event details:

Photonics Asia 2007: Sensors and Imaging
Beijing, China

Publication Date:

2007

Publisher DOI:

<http://dx.doi.org/10.1117/12.753772>

License:

<https://creativecommons.org/licenses/by-nc-nd/3.0/au/>

Link to license to see what you are allowed to do with this resource.

Downloaded from <http://hdl.handle.net/1959.4/43077> in <https://unsworks.unsw.edu.au> on 2024-04-24

An in-line in-fibre ring cavity multi-parameter sensor with a tuneable refractive index response.

Paul Childs, Ian Leung, Allan C.L. Wong, and Gang-Ding Peng

Photonics & Optical Communications Group
School of Electrical Engineering & Telecommunications,
University of New South Wales
Sydney 2052, Australia

Abstract

An in-line fibre ring cavity is fabricated by writing two blazed gratings next to each other to form a Fabry Perot cavity. A visibility of fringes as good as 0.032 in the reflection spectrum and 0.76 for transmission is obtained for the interference between the forward propagating guided mode and the reverse propagating ghost mode of the blazed grating. The ability to measure the external refractive index and the variability of this response with cavity length is demonstrated.

Keywords: Optical fibre sensors, blazed gratings, ring cavities.

1. Introduction

One of the key fields of research in the field of fibre optic sensing is multi-parameter sensing [1], i.e. being able to measure with the one fibre sensor a number of different parameters of the environment in which it is placed (such as strain, temperature, pressure, etc.). It is desirable for either of the situations where it is necessary to correct for an unwanted cross sensitivity of a sensor to another parameter (such as the strain-temperature cross sensitivity of a Fibre Bragg Grating (FBG) or a Long Period Grating (LPG)) or simply where being able to monitor a wider range of properties independently with the one system is useful.

The crude approach to multi-parameter sensing is to use a number of sensors at each location, each of which are designed to have a different ratio of the various sensitivities of the desired measurands. Examples of this include: packaging two FBGs such that one isn't subject to the one measurand, e.g. the strain field [2], writing FBGs having notably different wavelengths [3] or of different types (e.g. type I, type II, etc.) [4], writing FBGs on fibre having a different diameter [5] or different dopant concentration [6] and the use of two different fibre sensors, such as FBGs and LPGs [7-8], or FBGs and Fabry-Perot (FP) cavities [9].

A more advanced approach is to design a sensor that has a number of different properties intrinsic to itself, all of which can be used to independently determine several external properties for measurement. Some examples of such devices include: the use of Brillouin scattering [10] (which also allows for distributed sensing of the measurands to be determined at arbitrary distances along the length of the fibre), the use of two different polarisation modes of a fibre [11], an FBG where the first order and second order peak have different sensitivities [12], an FBG written on tapered fibre where, due to the taper, the bandwidth varies as well as the Bragg wavelength [13], and a regular LPG, as the different cladding modes have quite different sensitivities [14].

In this paper, blazed gratings will be investigated for their potential for use as a multi-parameter sensor. The particular gratings will make use of a Fabry Perot structure of the gratings which gives the additional property intrinsic to itself of the cavity quality factor (Q factor) allowing multi-parameter sensing, as well as meeting the spectral requirements that allow the grating to be multiplexed using Wavelength-frequency Division Multiplexing (W*DM) [15-16].

A blazed grating is a grating that has been written at an angle w.r.t. the cross-section of the fibre. This angle breaks the symmetry of the fibre such that light is reflected preferentially into the cladding modes of the fibre rather than simply being sent straight back into the guided mode. The spectrum of a blazed fibre grating is shown in figure 1. The Bragg peak corresponding to guided mode to guided mode reflection is the peak in the spectrum having the highest wavelength. The next strongest peak is the ghost mode (a highly resonant cladding mode). The remaining peaks are the resonant cladding modes of the blazed grating.

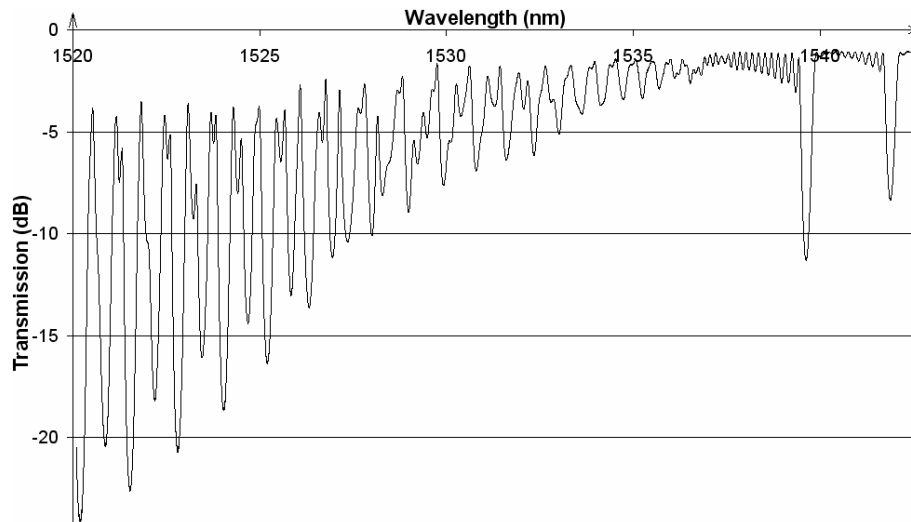


Figure 1. Spectrum of a blazed grating showing the peaks of its cladding modes, ghost mode and Bragg mode.

Blazed gratings have found applications as flattening filters for doped fibre amplifiers [17] and side tap gratings [18] where part of the light in the fibre at a certain wavelength or wavelength range is tapped off to monitor the light within the fibre without disrupting its propagation through the fibre.

Because of their cladding mode effects, blazed gratings allow the potential for multi-parameter sensing. The Bragg mode, the ghost mode and all the various cladding modes of blazed gratings have all the same wavelength sensitivity to strain and temperature as do standard FBGs. As such, wavelength measurements of the various modes doesn't allow for the ability to extend measurement from a single parameter type to a multi-parameter type.

Amplitude measurements on the other hand do. For the cladding modes, the visibility of the mode structure will depend on the external refractive index [19]. When the surrounding refractive index is significantly lower than that of the fibre cladding, the mode structure is clearly seen. When the refractive index matches that of the cladding, the resonant structure disappears altogether. A measure of the cladding mode structure can thus account for the refractive index of the surrounding medium. This still doesn't allow one to distinguish between strain and temperature, but it does, however, allow one to distinguish between the external refractive index and a combination of strain and temperature which can be determined by other means. The drawbacks to using such a sensor is that the cladding modes of a blazed grating occupy such a large amount of the spectrum it makes multiplexing them using Wavelength Division Multiplexing (WDM) over the C band impossible.

Long Period Gratings (LPGs) have also been used for multi-parameter sensing. The different strain and temperature responses of the various modes allow one to separate out these effects and monitor them independently [20]. LPGs can also be used to monitor the refractive index of the material surrounding the fibre as the effective index of the cladding modes (on which mode coupling for LPGs is based) is dependant on the external refractive index. A change in the surrounding refractive index will cause a wavelength shift and change the transmissivity of the cladding mode resonances [21]. Furthermore, the cladding modes will leach out due to the mismatch between the external refractive index and that of the cladding. Measuring the power in the cladding modes thus allows one to monitor the external refractive index. Such measurements can be made using cascaded LPGs [22]. One LPG couples light out into the cladding modes and the other one interferometrically couples some of it back in. Depletion of the cladding modes due to a refractive index mismatch will cause there to be less light to provide interference with the guided mode. However sensing with LPGs can be complicated due to their cross-sensitivity with a number of different measurands.

Another alternative is to make use of the ghost mode coupling. The term "ghost mode" was used by Jaynes to describe a highly resonant mode localised around a defect in a waveguide or a periodic structure [23]. Although somewhat misnamed for the case of fibre Bragg gratings, the defect around which this ghost mode is "localised" is the asymmetry of the grating itself, which is normally due to the blaze angle. The ghost mode has been shown to be due to coupling from the guided LP_{01} mode to either the backreflected LP_{11} mode [24] or potentially due to higher order modes [25]. This mode will eventually leak out leaving no evidence of it in reflection yet a dip in the transmission spectrum; hence its ghost-like quality.

The amount of coupling to the ghost and Bragg modes is dependant on the blaze angle of the grating. Erdogan and Sipe have shown that the coupling to the Bragg mode is fairly constant with increasing blaze angle until about 5° from whence it rapidly decreases; disappearing entirely at a certain critical angle [26]. The stronger the grating, the more sudden the change in coupling with blaze angle is. Fibres with different refractive index profiles, such as photosensitive cladding fibre, will have a different critical angle, not to mention an entirely different shape to the blaze angle response of the Bragg mode coupling coefficient [27]. The coupling with angle has also shown to be different for different modes [28]. Thus a blazed grating allows potential application for use as a multi-parameter sensor by measuring both the Bragg wavelength shift as well as the blaze angle from the amount of light coupling into the ghost mode [29].

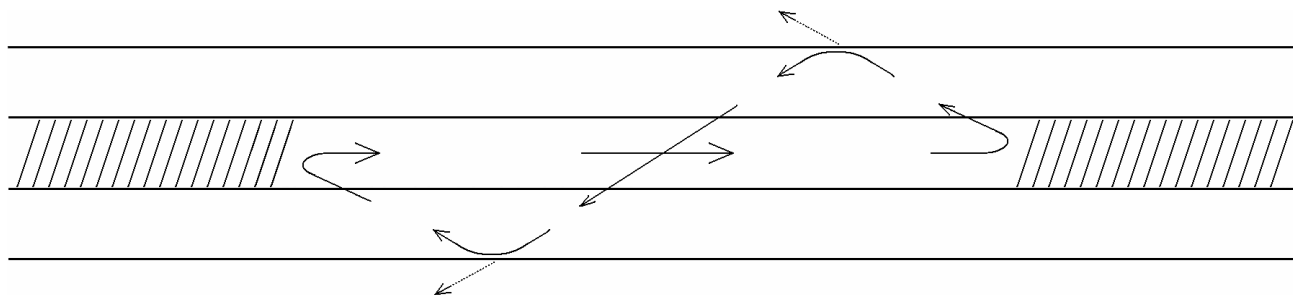


Figure 2. Structure of an in-line ring cavity showing core/cladding coupling due to the blazed gratings.

The ghost mode can be used to measure the surrounding refractive index, as was the case for the cladding modes, by making use of a resonant cavity structure, as shown in figure 2, where the level of interference between the two blazed gratings will change according to how much light is leaked out from the returning cladding mode. When the surrounding refractive index matches that of the cladding of the optical fibre, the cladding mode completely leaks out and thus there is no cladding mode to reach the second grating and cause interference. When the surrounding refractive index is sufficiently lower than that of the cladding of the optical fibre, the cladding mode propagates with hardly any loss and can thus recouple to the guided mode when it reaches the second blazed grating causing a good deal of interference. The amount of interference is measured by the visibility of fringes seen in the transmission loss band of the ghost mode spectrum. The relation between the visibility of fringes and the refractive index is strongly nonlinear, monotonically decreasing with refractive index going from the critical value of 1 to that of the cladding of the optical fibre. This effect can be tuned according to the spacing between the gratings. The larger the spacing the greater the attenuation of the cladding modes and thus the more rapidly the drop off of the visibility of fringes with external refractive index is.

As can be seen from figure 1, the cladding modes of a blazed grating are too strong to allow multiplexing using WDM with other blazed gratings. Due to the fringes that exist in the Bragg and ghost mode spectrum, another option would be to use WDM to multiplex sensors having different cavity lengths [15-16]. The visibility of fringes can be read directly from the corresponding window of the relevant sensor in the power spectrum of the Fourier domain spectrum of the ghost mode(s). Care must be taken, however, as spectral shadowing, when not properly compensated for, acts to reduce the amplitude in the Fourier domain thus giving a lower reading for the visibility of fringes than is actually occurring. This can be compensated by taking a reference measurement of the visibility of fringes of the Bragg mode by looking at its amplitude in the Fourier domain. Sensors that are designed to have the same transmission loss of the Bragg and ghost modes should give an equivalent amount of spectral shadowing effects to both the Bragg and ghost mode bands provided that no Bragg mode of one sensor overlaps a ghost mode of another sensor.

2. Experiment

Two Blazed Fabry Perot Gratings (BFPGs) were fabricated in highly photosensitive boron codoped germanosilicate fibre. The fibre had been hydrogen loaded by soaking it in hot hydrogen under pressure so as to increase its photosensitivity. The gratings were fabricated using holographic side exposure [30] by interfering the ± 1 orders of a phase mask on the fibre core [31]. The blaze of the grating was achieved by rotating the phase mask about its surface by the desired blaze angle. The blaze angle on the gratings was chosen to be approximately 4° ; at just a little below the critical blaze angle for this type of fibre so as to get a good reflectivity for both the Bragg and ghost modes. BFPG1 was fabricated by writing two gratings to give a cavity spacing of 15mm whereas for BFPG2 the cavity spacing was 30mm. The gratings were thermally aged by annealing them at 300°C for 5 minutes; leaving them in an oven overnight at 80°C allowed the hydrogen to outgas from the rest of the fibre.

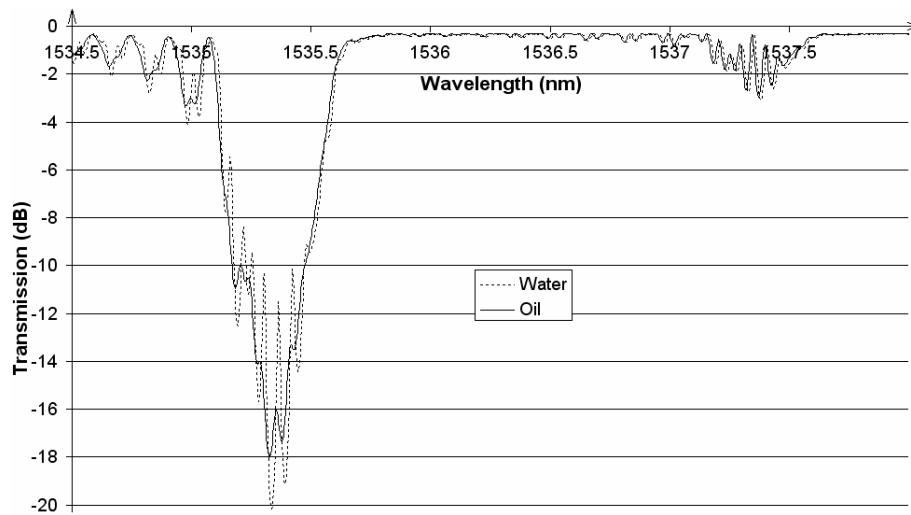


Figure 3. Transmission spectrum obtained when immersing BFPG1 (15mm cavity) in water and in oil.

Each grating was in turn immersed in water (refractive index = 1.33) and paraffin oil (refractive index = 1.42) and the transmission spectrum monitored. The results are shown in figure 3 and figure 4 for BFPG1 and BFPG2 respectively. It can be seen that the visibility of fringes remains unchanged for the Bragg peak no matter what medium the fibre is immersed into. Such is not the case, however, for the ghost mode resonance. Whereas there is still a good degree of visibility of fringes to be seen when immersed in water, paraffin oil almost washes them out completely. The visibility of fringes for the transmission spectrum in figure 3 is calculated to be 0.76; also giving an associated visibility of fringes in reflection of 0.032 showing that the cavity is only very weakly resonant, yet still with the ability to obtain good fringe contrast using transmission measurements.

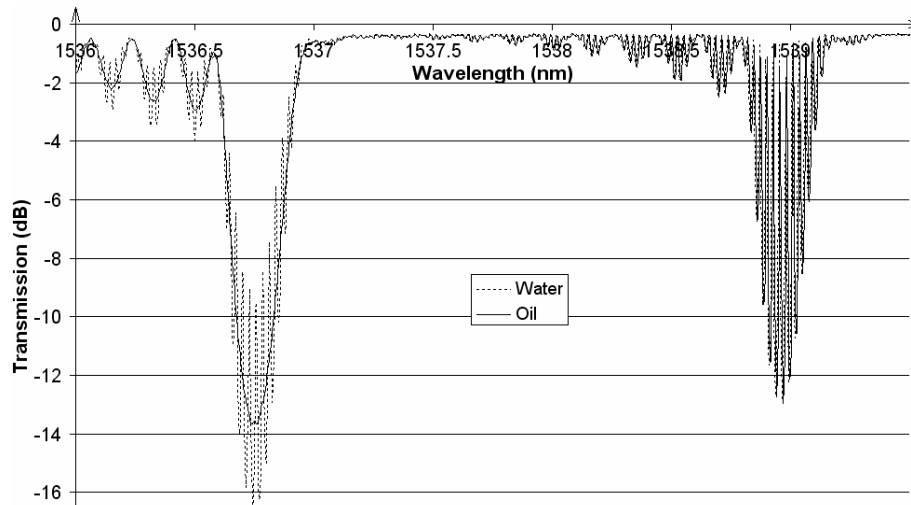


Figure 4. Transmission spectrum obtained when immersing BFPG2 (30mm cavity) in water and in oil.

BFPG1 and BFPG2 were then immersed in 80% and 40% Brix sugar solutions respectively. The transmission spectra of the gratings were monitored as the solutions were gradually diluted. The external refractive index was calculated from calibration tables for known sugar solution concentrations. Two separate Fourier transforms were applied to the data sets around the ghost peak and the Bragg peak. The peak in the magnitude spectrum corresponding to the wavelength frequency of the interference was taken for both cases. The ratio of this value for the ghost peak and the Bragg peak gave the visibility ratio which is plotted as a function of the external refractive index in figure 5 and figure 6 for BFPG1 and BFPG2 respectively. The more rapid response change of the longer cavity BFPG2 at lower external refractive indexes

can be clearly seen from these figures. Thus a measure of tuneability of the response has been achieved through varying the size of the cavity.

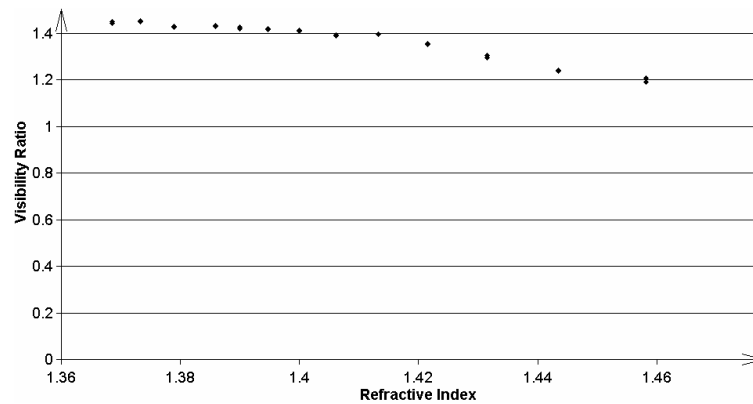


Figure 5. Response of the visibility of fringes of the ghost mode to the external refractive index for BFPG1.

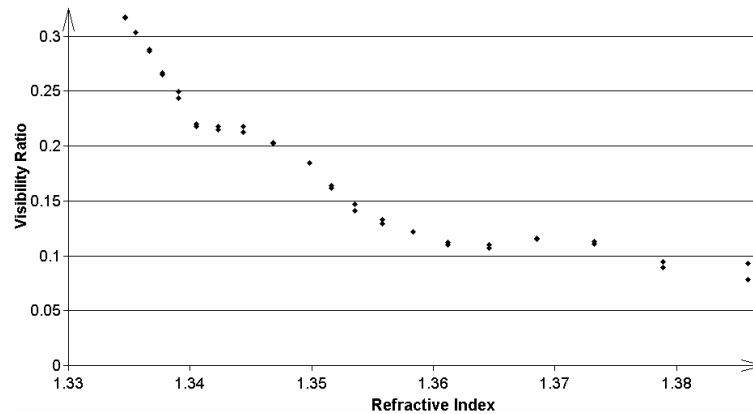


Figure 6. Response of the visibility of fringes of the ghost mode to the external refractive index for BFPG2.

3. Conclusion

Two in-line in-fibre ring cavities were fabricated having resonances giving visibility of fringes of 0.032 in reflection and 0.76 in transmission. The ability of these to be used as a multi-parameter sensor was shown by making use of its spectral response to the external refractive index. Tuneability of this response was obtained by varying the cavity length.

References

1. O. Frazão, L.A. Ferreira, F.M. Arújo, and J.L. Santos "Applications of fiber optic grating technology to multi-parameter measurement" in *Fiber Integr. Opt.*, Vol. 24, No. 3-4, pp. 227-244 (2005).
2. A.D. Kersey, T.A. Berkoff, and W.W. Morey "Fibre optic Bragg grating strain sensor with drift compensated high resolution interferometric wavelength shift detection" in *Opt. Lett.*, Vol. 18, No. 1, pp. 72-74 (1993).
3. M.G. Xu, J.L. Archambault, L. Reekie, and J.P. Dakin "Discrimination between strain and temperature effects using dual-wavelength fibre grating sensors" in *Electron. Lett.*, Vol. 30, No. 13, pp. 1085-1087 (1994).
4. O. Frazão, M.J.N. Lima, and J.L. Santos "Simultaneous measurement of strain and temperature using type I and type IIA fibre Bragg gratings" in *J. Opt. A: Pure Appl. Opt.*, Vol. 5, No. 3, pp. 183-185 (2003).
5. S.W. James, M.L. Dockney, and R.P. Tatum "Simultaneous independent temperature and strain measurement using in-fibre Bragg grating sensors" in *Electron. Lett.*, Vol. 32, No. 12, pp. 1133-1134 (1996).

6. P.M. Cavaleiro, F.M. Araújo, L.A. Ferreira, J.L. Santos, and F. Farahi "Simultaneous measurement of strain and temperature using Bragg gratings written in germanosilicate and boron-codoped germanosilicate fibers" in IEEE Photon. Technol. Lett., Vol. 11, No. 12, pp. 1635-1637 (1999).
7. H.J. Patrick, G.M. Williams, A.D. Kersey, J.R. Pedrazzani, and A.M. Vengsarkar "Hybrid fiber Bragg grating/long period fiber grating sensor for strain/temperature discrimination" in IEEE Photon. Technol. Lett. Vol. 8, No. 9, pp. 1223-1225 (1996).
8. B.O. Guan, H.Y. Tam, X.M. Tao, and X.Y. Dong "Simultaneous strain and temperature measurement using a superstructure fiber bragg grating" in IEEE Photon. Technol. Lett., Vol. 12, No. 6, pp. 675-677 (2000).
9. L.A. Ferreira, A.B. Lobo Ribeiro, J.L. Santos, and F. Farahi "Simultaneous measurement of displacement and temperature using a low finesse cavity and a fiber Bragg grating" in IEEE Photonics Technol. Lett., Vol. 8, No. 11, pp. 1519-1521 (1996).
10. J. Smith, A. Brown, M. deMerchant, and X. Bao "Simultaneous distributed strain and temperature measurement" in Appl. Opt., Vol. 38, No. 25, pp. 5372-5377 (1999).
11. A.M. Vengsarkar, W.C. Michie, L. Jankovic, B. Culshaw, and R.O. Claus "Fiber optic sensor for simultaneous measurement of strain and temperature" in Proc. SPIE, Vol. 1367, pp. 249-260 (1991).
12. G.P. Brady, K. Kalli, D.J. Webb, D.A. Jackson, L. Reekie, and J.L. Archambault "Simultaneous measurement of strain and temperature using the first and second-order diffraction wavelengths of Bragg gratings" in Proc. IEEE, Optoelectron., Vol. 144, No. 3, pp. 156-161 (1997).
13. M.G. Xu, L. Dong, L. Reekie, J.A. Tucknott, and J.L. Cruz "Temperature-independent strain sensor using a chirped Bragg grating in a tapered optical fibre" in Electron. Lett., Vol. 31, No. 10, pp. 823-825 (1995).
14. V. Bhatia, D. Campbell, and R.O. Claus "Simultaneous strain and temperature measurement with long-period gratings" in Opt. Lett., Vol. 22, No. 9, pp. 648-650 (1997).
15. P. Childs "An FBG sensing system utilizing both WDM and a novel harmonic division scheme" in J. Lightw. Technol., Vol. 23, No. 1, pp. 348-354, (2005); "Erratum" Vol. 23, No. 2, pp. 931, (2005).
16. P. Childs, T. Whitbread, and G.D. Peng "Spectrally coded multiplexing in a strain sensor system based on carrier-modulated fibre Bragg gratings" in Proc. SPIE, Vol. 5634, pp. 204-210 (2005).
17. R. Kashyap, R. Wyatt, and R.J. Campbell "Wideband gain flattened Erbium fibre amplifier using a photosensitive fibre blazed grating" in Electron. Lett., Vol. 29, No. 2, pp. 154-156 (1993).
18. J.L. Wagener, T.A. Strasser, J.R. Pedrazzani, and J. deMarco "Fiber grating optical spectrum analyzer tap" in Proc. IOOC/ECOC, Vol. 5, pp. 65-68 (1997).
19. T. Erdogan "Cladding-mode resonances in short- and long-period fiber grating filters" in J. Opt. Soc. Am. A, Vol. 14, No. 8, pp. 1760-1773 (1997); "Erratum" Vol. 17, No. 11, pp. 2113 (2000).
20. V. Bhatia, D. Campbell, and R.O. Claus "Simultaneous strain and temperature measurement with long-period gratings" in Opt. Lett., Vol. 22, No. 9, pp. 648-650 (1997).
21. B.H. Lee, Y. Liu, S.B. Lee, S.S. Choi, and J.N. Jang "Displacements of the resonant peaks of a long-period fiber grating induced by a change of ambient refractive index" in Opt. Lett., Vol. 23, No. 22, pp. 1769-1771 (1996).
22. E.M. Dianov, S.A. Vasiliev, A.S. Kurkov, O.I. Medvedkov, and V.N. Protopopov "in-fiber Mach-Zehnder interferometer based on a pair of long-period gratings" in Proc. ECOC, pp. 65-68 (1996).
23. E.T. Jaynes "Ghost modes in imperfect waveguides" in Proc. IRE, Vol. 46, pp. 416-418 (1958).
24. W.W. Morey, G. Meltz, J.D. Love, and S.J. Hewlett "Mode-coupling characteristics of UV-written Bragg gratings in depressed-cladding fibre" in Electron. Lett., Vol. 30, No. 9, pp. 730-732 (1994).
25. S.J. Hewlett, J.D. Love, G. Meltz, T.J. Bailey, and W.W. Morey "Cladding-mode coupling characteristics of Bragg gratings in depressed-cladding fibre" in Electron. Lett., Vol. 31, No. 10, pp. 820-822 (1995).
26. T. Erdogan, and J.E. Sipe "Tilted fiber phase gratings" in J. Opt. Soc. Am. A, Vol. 13, No. 2, pp. 296-313 (1996).
27. L. Brillard, D. Pureur, J.F. Bayon, and E. Delevaque "Slanted gratings UV-written in photosensitive cladding fibre" in Electron. Lett., Vol. 35, No. 3, pp. 234-236 (1999).
28. L. Dong, B. Ortega, and L. Reekie "Coupling Characteristics of Cladding Modes in Tilted Optical Fiber Bragg Gratings" in Appl. Opt., Vol. 37, No. 22, pp. 5099-5105 (1998).
29. S. Baek, Y. Jeong, and B. Lee "Characteristics of short-period blazed fiber Bragg gratings for use as macro-bending sensors" in Appl. Opt., Vol. 41, No. 4, pp. 631-636 (2002).
30. G. Meltz, W.W. Morey, and W.H. Glenn "Formation of Bragg gratings in optical fibers by a transverse holographic method" in Opt. Lett. Vol. 14, No. 15, pp. 823-825 (1989).
31. D.Z. Anderson, V. Mizrahi, T. Erdogan, and A.E. White "Production of In-Fibre Gratings Using a Diffractive Optical Element" in Electron. Lett., Vol. 29, No. 6, pp. 566-568 (1993).